Tuning heavy fermion systems into quantum criticality by magnetic field

Philipp Gegenwart, J. Custers, T. Tayama, K. Tenya, C. Geibel, G. Sparn, N. Harrison, P. Kerschl, D. Eckert, K.-H. Müller, F. Steglich

Angaben zur Veröffentlichung / Publication details:

Gegenwart, Philipp, J. Custers, T. Tayama, K. Tenya, C. Geibel, G. Sparn, N. Harrison, et al. 2003. "Tuning heavy fermion systems into quantum criticality by magnetic field." *Journal of Low Temperature Physics* 133 (1/2): 3–15. https://doi.org/10.1023/a:1025624831341.

Tuning Heavy Fermion Systems into Quantum Criticality by Magnetic Field

P. Gegenwart,[1] J. Custers,[1] T. Tayama,[1] K. Tenya,[1] C. Geibel,[1] G. Sparn,[1] N. Harrison,[2] P. Kerschl,[3] D. Eckert,[3] K.-H. Müller,[3] and F. Steglich[1]

[1] *Max-Planck Institute for Chemical Physics of Solids, D-01187 Dresden, Germany*
E-mail: gegenwart@cpfs.mpg.de
[2] *Los Alamos National Laboratory, Los Alamos, New Mexico 87545, USA*
[3] *Leibniz Institute for Solid State and Materials Research, D-01187 Dresden, Germany*

We discuss a series of thermodynamic, magnetic, and electrical transport experiments on the two heavy fermion compounds $CeNi_2Ge_2$ and $YbRh_2Si_2$ in which magnetic fields, B*, are used to tune the systems from a non-Fermi liquid (NFL) into a field-induced FL state. Upon approaching the quantum-critical points from the FL side by reducing* B *we analyze the heavy quasi-particle (QP) mass and QP-QP scattering cross sections. For $CeNi_2Ge_2$ the observed behavior agrees well with the predictions of the spin-density wave (SDW) scenario for three-dimensional (3D) critical spin-fluctuations. By contrast, the observed singularity in $YbRh_2Si_2$ cannot be explained by the itinerant SDW theory for neither 3D nor 2D critical spinfluctuations. Furthermore, we investigate the magnetization* M(B) *at high magnetic fields. For $CeNi_2Ge_2$ a metamagnetic transition is observed at 43 T, whereas for $YbRh_2Si_2$ a kink-like anomaly occurs at 10 T in* M vs B *(applied along the easy basal plane) above which the heavy fermion state is completely suppressed.*

***KEY WORDS*:** heavy fermion; magnetic field; $CeNi_2Ge_2$; $YbRh_2Si_2$.

1. INTRODUCTION

Quantum critical points (QCPs) are of extensive current interest to the physics of correlated electrons, as the proximity to a QCP provides a route towards non-Fermi liquid (NFL) behavior. While a broad range of correlated electron materials are being studied in this context, heavy fermion (HF) metals have been playing an especially important role since a growing list of them have been found to explicitly display a magnetic

QCP.[1] HF metals contain a dense lattice of certain lanthanide ($4f$) or actinide ($5f$) ions which are, at sufficiently low temperatures ($T \ll T_K$, T_K: Kondo temperature), strongly coupled by the conduction electrons, yielding the formation of heavy quasiparticles (QP). They are highly suited to study quantum-critical behavior since they can be tuned continuously from an antiferromagnetic (AF) to a paramagnetic metallic state by the variation of a single parameter, i.e., the strength of the $4f$-conduction electron hybridization g, which can be modified by the application of either external pressure or chemical substitution.

The origin of NFL behavior in HF systems has been studied intensively in the past decade but is still unclear up to now.[1] In particular, two different scenarios are discussed for the QCP, where long-range AF order emerges from the HF state; one in which NFL behavior arises from Bragg diffraction of the electrons off a critical spin-density wave (SDW),[3–5] the other one in which the bound-state structure of the composite heavy fermions breaks up at the QCP resulting in a collapse of the effective Fermi temperature.[2,6] In the SDW scenario, assuming three-dimensional (3D) spinfluctuations, singular scattering occurs only along certain "hot lines" connected by the vector $\mathbf{q}$ of the nearby AF order while the remaining Fermi surface still behaves as a Landau Fermi liquid (LFL). Therefore, the low-temperature specific heat coefficient $C(T)/T$ that measures the QP mass is expected to show an anomalous temperature dependence $C(T)/T = \gamma_0 - \alpha\sqrt{T}$, but remains finite at the QCP.[5] A diverging QP mass, as evident from the $C(T)/T \propto \log(T_0/T)$ behavior found, e.g., in the prototypical system $CeCu_{6-x}Au_x$ for $x_c = 0.1$ (Ref. 7), would arise only if truly 2D critical spinfluctuations render the entire Fermi surface "hot."[8] On the other hand, measurements of the inelastic neutron scattering on $CeCu_{5.9}Au_{0.1}$[9] showed that the critical component of the spin fluctuations is almost momentum independent leading to the proposal of the locally critical scenario.[6,9] Since T-dependent measurements at the QCP alone provide no information on how the heavy quasiparticles decay into the quantum critical state it is necessary to tune the system away from the magnetic instability in the LFL state and to follow the QP properties upon approaching the QCP. We will show that magnetic fields can be used for this purpose.

The aim of this article is to review a number of experiments on the HF systems $CeNi_2Ge_2$[10] (Sec. 2) and $YbRh_2Si_2$[11] (Sec. 3) that both crystallize in the tetragonal $ThCr_2Si_2$ structure. They are ideally suited to study AF QCPs since they are located very near to the magnetic instability, and since the effect of disorder is minimized in these high quality single crystals with very low residual resistivities. We focus on low temperature specific heat, C, and electrical resistivity, ρ, measurements at various magnetic fields that

allow to follow the QP mass and QP-QP scattering cross section upon approaching the QCP from the field-induced FL side. Furthermore, the high field dc-magnetization $M(B)$ has been measured for both systems in order to investigate the suppression of the Kondo effect by the polarization of the magnetic moments.

2. $CeNi_2Ge_2$

As first reported by Knopp *et al.*,[12] $CeNi_2Ge_2$ is one of the very few HF systems exhibiting a non-magnetically ordered, non-superconducting ground state. From both the low temperature specific heat coefficient of about 0.35 $JK^{-2}mol^{-1}$ and the flat minimum at $T \approx 30$ K in the temperature dependence of the quasielastic line width $\Gamma(T)$, measured by inelastic neutron scattering, a Kondo temperature of 30 K has been deduced.[12] Furthermore, a broad maximum is observed at 30 K for the magnetic susceptibility $\chi(T)$ measured along the magnetic easy direction parallel to the crystallographic c-axis, resembling the prototypical Kondo-lattice system $CeRu_2Si_2$ ($T_K = 10$ K).[14] In contrast to $CeRu_2Si_2$, for $CeNi_2Ge_2$ the closer inspection of the low temperature thermodynamic and transport properties, as will be discussed below, revealed pronounced NFL behavior at temperatures well below T_K.[10] The NFL effects are clearly related to a very nearby magnetic instability: increasing the lattice parameter by isoelectronic substitution of the Ni by the larger Pd atomes in $Ce(Ni_{1-x}Pd_x)_2Ge_2$ induces long-range AF order below $T_N = 2$ K for $x = 0.2$ (Ref. 13). The extrapolation of $T_N(x)$ towards zero temperature suggests a very small critical concentration x_c.

The low temperature specific heat coefficient measured with a high-quality polycrystalline $CeNi_2Ge_2$ sample[10] is plotted in Fig. 1 on a logarithmic temperature scale. Instead of being constant, as expected for a FL, $C(T)/T$ strongly increases upon cooling from 6 K to 0.4 K. Similar behavior has been reported in Refs. 12, 15–18. Below 2 K, this increase can be well described by $C(T)/T = \gamma_0 - c\sqrt{T}$ with $\gamma_0 = 0.43$ $JK^{-2}mol^{-1}$ (see dotted line in Fig. 1). Such a temperature dependence has been predicted by the 3D-SDW theory for systems at an AF QCP.[3–5]

The application of magnetic fields to $CeNi_2Ge_2$ is found to gradually reduce the low-T specific heat coefficient (see Fig. 1) and induces LFL behavior. For $B \geqslant 2$ T a constant $\gamma_0(B) = C(T, B)/T$ value is observed at the lowest temperatures. Upon warming, $C(T, B)/T$ passes through a broad maximum at a characteristic temperature $T^\star(B)$ that increases linearly with increasing magnetic field.[10, 15, 16] In the inset of Fig. 1, we analyze the magnetic field dependence of the low-T specific heat coefficient

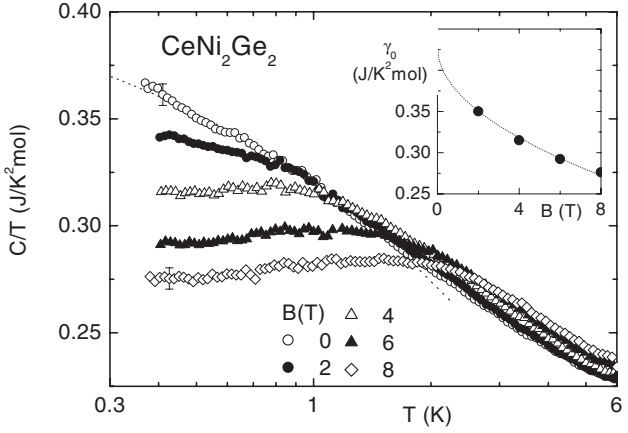

Fig. 1. Low temperature specific heat of $CeNi_2Ge_2$ as C/T vs. T (on a logarithmic scale) at $B = 0$ and differing magnetic fields. Dotted line indicates $C(T)/T = \gamma_0 - \beta\sqrt{T}$ using $\gamma_0 = 0.43\,\mathrm{JK^{-2}mol^{-1}}$ and $\beta = 0.11\,\mathrm{JK^{-5/2}mol^{-1}}$. Inset displays field dependence of coefficient $\gamma_0(B)$ characterizing the field-induced FL state. Dotted line represents $\gamma_0(B) = \gamma_0 - \beta'\sqrt{B}$ with $\beta' = 0.055\,\mathrm{JK^{-2}T^{-1/2}mol^{-1}}$.

$\gamma_0(B)$ that measures the heavy quasiparticle mass in the LFL regime. Upon reducing the magnetic field towards zero, we are able to follow the evolution of this true $T = 0$ property upon tuning the system towards the QCP. We observe (see inset Fig. 1) that the field dependence of the specific heat coefficient $\gamma_0(B)$ (at $T = 0$) is very similar to the temperature dependence of C/T at $B = 0$.

Next we turn to the low temperature resisitivity of $CeNi_2Ge_2$. In Fig. 2a three polycrystalline samples with different residual resistivities are compared.[10] The "standard-quality" sample with $\rho_0 = 2.7\,\mu\Omega\mathrm{cm}$ follows $\Delta\rho(T) = \rho - \rho_0 = \beta T^{1.5}$ for more than two decades in temperature between 20 mK and 2.5 K, in perfect agreement with the 3D-SDW prediction.[3–5] For high-quality samples with a ten times lower residual resistivity, the exponent is slightly smaller, i.e., deviates even stronger from FL behavior. A similar observation has been made on slightly-off stoichiometric $Ce_{1+x}Ni_{2+y}Ge_{2+z}$ polycrystals where the Ni-Ge ratio was varied by a few at-%. Exponents of $\epsilon = 1.5$ for $\rho_0 \gtrsim 3\,\mu\Omega\mathrm{cm}$ and $1.3 \leqslant \epsilon < 1.5$ for $0.17\,\mu\Omega\mathrm{cm} \leqslant \rho_0 < 3\,\mu\Omega\mathrm{cm}$ have been found.[19] The onset of superconductivity at very low tempeatures (Fig. 2b) observed by several different investigations[10, 16, 19–21] has not been detected by any bulk probe so far.

As demonstrated for a high-quality sample in Fig. 3, the application of magnetic fields forces the low-temperature resistivity to turn into a $\Delta\rho = A(B)\,T^2$ behavior consistent with the specific heat results discussed

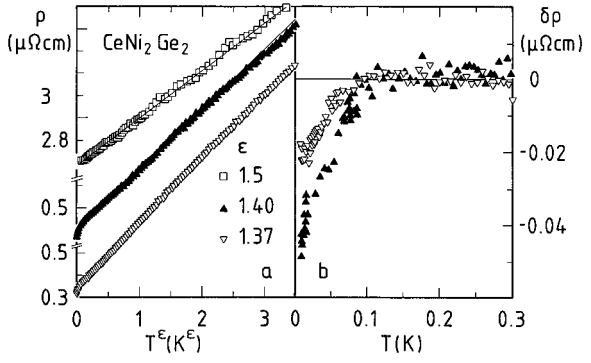

Fig. 2. Electrical resistivity as a function of temperature for three $CeNi_2Ge_2$ samples with $\rho_0 = 2.7$ μΩcm (□), 0.43 μΩcm (▲), and 0.34 μΩcm (▽) as ρ vs. T^ϵ with different exponents ϵ (a) and $\delta\rho = \rho - (\rho_0 + \beta T^\epsilon)$ vs. T (b).

above. The cross-over temperature, detected for the three different polycrystals, increases proportionally to $B^{0.65}$ (Fig. 4a), whereas the coefficient $A(B)$ in the LFL regime diverges as $A(B) \propto B^{-0.6}$ (Fig. 4b). Again, this field dependence of the $T = 0$ scattering cross-section for QP-QP scattering is very similar to the temperature dependence of the corresponding $A(T) = \Delta\rho(T)/T^2 \propto T^{-0.5}$ at $B = 0$. Thus, in the approach to the QCP, both as a function of T and B, the QP mass and QP-QP scattering cross section grow consistent with the predictions of the SDW scenario for 3D critical AF spinfluctuations.

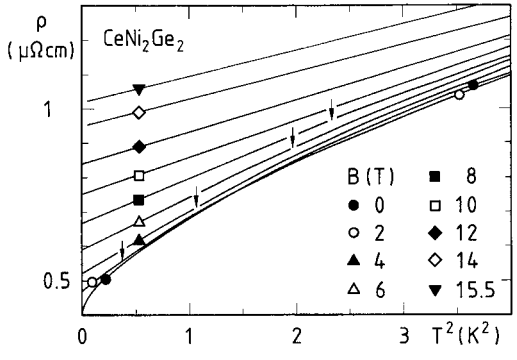

Fig. 3. Magnetic field dependence of $\rho(T)$ of a high-quality $CeNi_2Ge_2$ sample ($\rho_0 = 0.43$ μΩcm) as ρ vs. T^2 in fields up to 15.5 T. Arrows indicate limiting temperature of the validity range of the T^2 law.

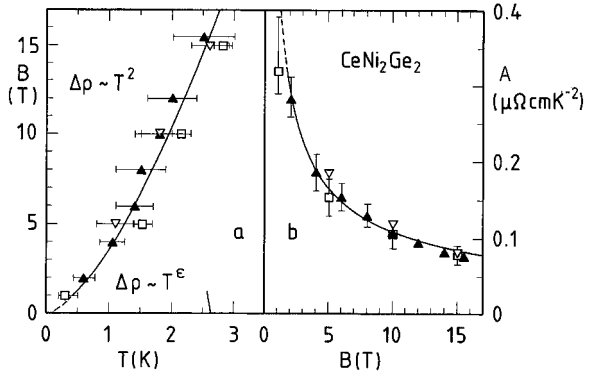

Fig. 4. (a) B-T phase diagram for $CeNi_2Ge_2$ with existence ranges of non-Fermi liquid ($\Delta\rho \sim T^{\epsilon}$, $1.37 \leqslant \epsilon \leqslant 1.5$) and Fermi liquid ($\Delta\rho = A(B)\,T^2$) behavior. Symbols to characterize three different $CeNi_2Ge_2$ samples are the same as in Fig. 2. Solid line represents $B \propto T^{1.54}$. (b) Field dependence of coefficient A. Solid line indicates $A \propto B^{-0.6}$.

The specific heat and electrical resistivity measurements indicate that the quantum-critical fluctuations, responsible for the NFL behavior in $CeNi_2Ge_2$, are extremely sensitive to the application of magnetic fields. Fields of the order of 1 T only are sufficient to induce a LFL state with a strongly field-dependent QP mass and QP-QP scattering cross section. On the other hand, the magnetic fields necessary to suppress the Kondo effect by a polarization of the magnetic moments are much larger. We studied the high-field magnetization $M(B)$ of $CeNi_2Ge_2$ at the Dresden pulsed-field facility up to 50 T (Fig. 5). In order to minimize the effect of eddy currents, induced by the large dB/dt rate in this high-purity material with very low residual resistivity, the sample has been powdered and the grains have been mixed with insulating paraffin. A steady field of 5 T, applied above the paraffin's melting temperature, has been used to orient the powder. After subsequent cooling, the susceptibility of the oriented powder agreed well with that for a single crystal measured along the easy direction along the c-axis. As shown in Fig. 5, $M(B)$ shows a step-like anomaly around 43 T, corresponding to a peak in the susceptibility that grows in magnitude and sharpens upon reducing the temperature. A similar behavior has also been reported by Fukuhara *et al.*[22] who measured an (unoriented) free powder sample. They proposed that the origin of this metamagnetic anomaly is related to that observed in $CeRu_2Si_2$[14] and other HF systems. Apparently, this metamagnetic transition is clearly separated from the quantum-critical behavior observed in very small magnetic fields $B < 1$ T.

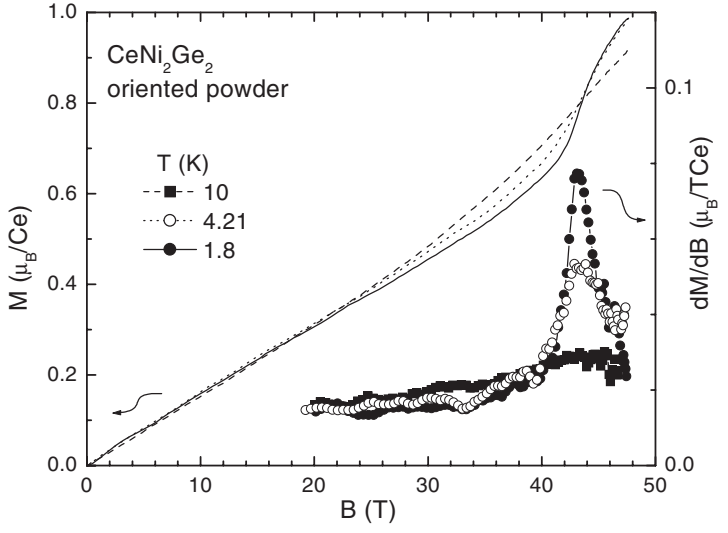

Fig. 5. Magnetization, M (right axis) and susceptibility, dM/dB (left axis), of $CeNi_2Ge_2$ measured in pulsed fields at various temperatures on an oriented powder sample ($B \parallel c$). These data were obtained at the IFW in Dresden.

3. $YbRh_2Si_2$

We next consider the HF metal $YbRh_2Si_2$ for which pronounced NFL phenomena, i.e., a logarithmic divergence of $C(T)/T$ and a quasi-linear T-dependence of the electrical resistivity below 10 K, have been observed above a low-lying AF phase transition.[11] We use magnetic fields to tune the system through the QCP. This investigation was motivated by previous studies on field-induced NFL behavior in the doped AF systems $CeCu_{6-x}Ag_x$[23,24] and $YbCu_{5-x}Al_x$.[25] $YbRh_2Si_2$ is best suited to tune into quantum criticality by magnetic field, because (i) the ordering temperature $T_N = 70$ mK is the lowest among all undoped HF systems at ambient pressure, (ii) already a very small critical magnetic field $B_c = 0.06$ T is sufficient to push T_N towards zero temperature, and (iii) the influence of disorder is minimized in very clean single crystals with a residual resistivity of about 1 μΩcm.

We first discuss the magnetic properties of $YbRh_2Si_2$ (Fig. 6). At high temperatures ($T \geqslant 200$ K) the magnetic susceptibility of $YbRh_2Si_2$ measured along both major crystallographic directions (a and c) follows a Curie–Weiss law with effective magnetic moments very close to the value of free Yb^{3+} ($\mu_{\text{eff}} = 4.5\mu_B$); but due to the strong magnetocrystalline anisotropy there is a marked difference in the respective extrapolated values for

the Weiss temperatures $\Theta^a \approx -9$ K and $\Theta^c \approx -180$ K.[26] At $T = 2$ K the magnetic susceptibility measured along the basal plane is about 20 times larger compared to the value measured with applied field parallel to the c-axis. Fig. 6a is indicating that in $YbRh_2Si_2$ the Yb^{3+} moments form an "easy-plane" square lattice with a strongly anisotropic response. This anisotropy is also reflected in the isothermal magnetization (Fig. 6c): Whereas for fields applied in the easy plane a strongly nonlinear response is observed with a polarized moment of 1 μ_B/Yb at 10 T, the magnetization along the hard (c-axis) is much smaller and almost perfectly linear up to 56 T. No indication of any anomaly is observed for this field orientation.[27] On the other hand, a clear kink is visible in the easy-plane magnetization at 10 T. Corresponding anomalies have been observed in the isothermal magnetoresistance and magnetostriction as well.[28] According to specific heat and electrical resistivity measurements as a function of temperature, the HF state is completely suppressed for $B \gtrsim 10$ T and the system behaves as a metal with polarized local magnetic moments.[28] In the following, we will focus on the quantum-critical behavior in small fields, well below 10 T.

Temperature-dependent measurements of the ac-susceptibility[11,29] and electrical resistivity[29] have revealed that the AF order at $T_N = 70$ mK (Fig. 6b) is completely suppressed by a critical magnetic field B_c of 0.06 T,

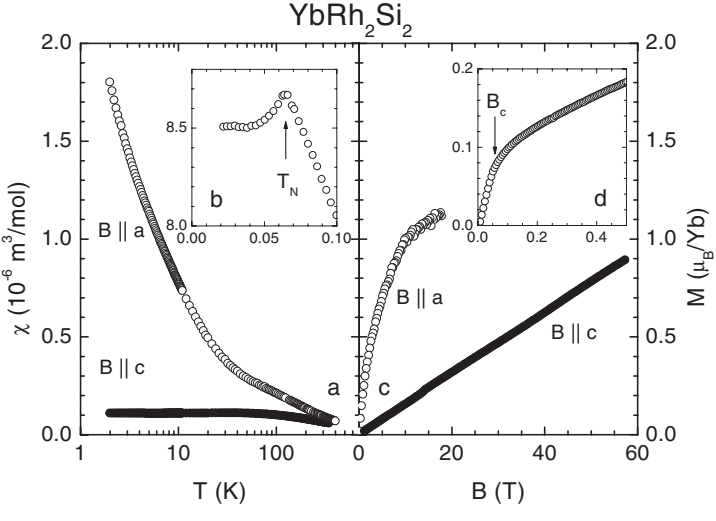

Fig. 6. Magnetic properties of $YbRh_2Si_2$ in fields applied along the a- (◦) and c-axis (•): $\chi = M/B$ vs. T in $B = 1$T (a). Inset (b) displays low temperature ac-susceptibility for $B \| a$ at zero dc field. (c): isothermal magnetization M vs. B at 2 K. Pulsed-field data have been obtained at the NHMFL in Los Alamos. Inset (d) displays low-field region for $B \| a$ at $T = 40$ mK.

applied in the easy plane, only. The isothermal magnetization, measured at a temperature $T \ll T_N$, shows a kink at B_c, indicative for a continuous second-order phase transition (Fig. 6d). The value of the ordered magnetic moment derived from the magnetic entropy[29] and μSR experiments[30] is well below 0.1 μ_B/Yb, in accordance with the small $M(B_c)$. Thus a large fraction of the local moments appears to remain fluctuating within the easy plane in the AF ordered state. Their continuous polarization gives rise to a strong curvature in $M(B)$ for $B > B_c$. The low value of B_c indicates that the AF and field-aligned states are nearly degenerate in $YbRh_2Si_2$. Thus, low-lying ferromagnetic ($\mathbf{q} = 0$) fluctuations are expected as indeed found by recent ^{29}Si-NMR experiments.[31]

In Fig. 7 we show the evolution of the low-temperature resistivity upon applying magnetic fields along and perpendicular to the easy magnetic plane. At small magnetic fields the Néel temperature, determined from the maximum value of $d\rho/dT$, shifts to lower temperatures and vanishes at $B_c = 0.06$ T (in the easy magnetic plane) and 0.66 T ($B \parallel c$). At $B = B_c$, the resistivity follows a linear T-dependence down to the lowest accessible temperature of about 20 mK. This observation provides striking evidence for field-induced NFL behavior at the critical magnetic fields applied along both crystallographic directions.[29] Fields larger than B_c induce LFL behavior in the specific heat coefficient $C(T)/T = \gamma_0(B)$, electrical resistivity

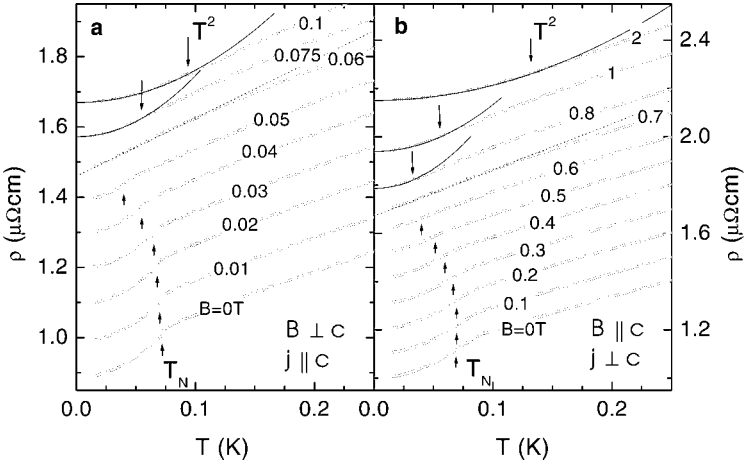

Fig. 7. Low-temperature electrical resistivity of $YbRh_2Si_2$ at varying magnetic fields applied perpendicular (a) and along the c-axis (b). For clarity the different curves in $B > 0$ were shifted subsequently by 0.1 μΩcm. Up- and down-raising arrows indicate T_N and upper limit of T^2 behavior, respectively. Dotted and solid lines represent $\Delta\rho \sim T^\epsilon$ with $\epsilon = 1$ and $\epsilon = 2$, respectively.

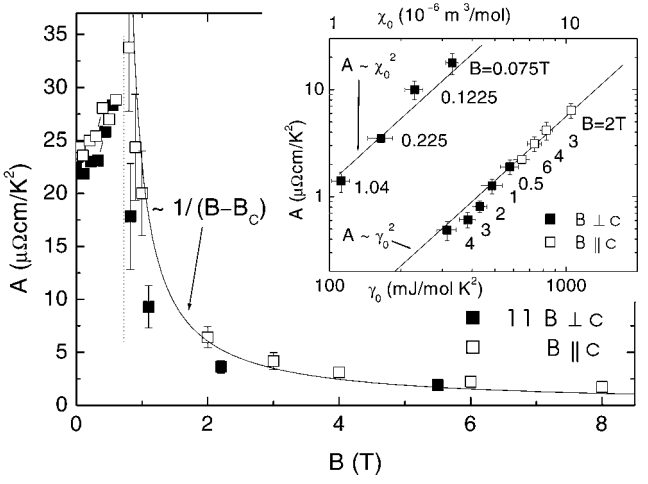

Fig. 8. Coefficient $A = \Delta\rho/T^2$ of $YbRh_2Si_2$ vs. field B. Data for B perpendicular to the c-direction have been multiplied by 11. Dashed line marks B_c, solid line represents $(B-B_c)^{-1}$. Inset shows double-log plot of A vs. γ_0 and A vs. χ_0 for different magnetic fields. Solid lines represent $A/\gamma_0^2 = 5.8\cdot10^{-6}$ μΩcm(Kmol/mJ)^2 and $A/\chi_0^2 = 1.25\cdot10^{12}$ μΩcmK^{-2}/(m^3/mol)^2.

$\Delta\rho(T) = A(B)\,T^2$, and magnetic susceptibility $\chi(T) = \chi_0(B)$ below a characteristic temperature $T^\star(B)$ that increases linearly with increasing B (Ref. 29).

In the following, we analyze the evolution of these coefficients that characterize the field-induced LFL state upon reducing B towards the QCP at B_c. As shown in Fig. 8, the coefficient $A(B)$ diverges as $(B-B_c)^{-1}$. Since $A(B)$ measures the QP-QP scattering cross section, this divergence indicates that the whole Fermi surface undergoes singular scattering at the field-induced QCP.[29] Furthermore, as shown in the inset of Fig. 8, we observe a constant "Kadowaki–Woods" ratio $K = A/\gamma_0^2$ with a value typical for other HF systems[32] in $B \geqslant 0.5$ T. Since A not only scales with γ_0^2 but also with χ_0^2, not only the QP mass but also the Pauli susceptibility diverges upon approaching the QCP. The very large Sommerfeld–Wilson ratio $R = (\chi_0/\gamma_0)(\pi^2 k_B^2/\mu_0\mu_{\text{eff}}^2)$ of about 14 ($\mu_{\text{eff}} = 1.4\mu_B$) indicates the strongly enhanced ($\mathbf{q} = 0$) susceptibility in the field-aligned state of $YbRh_2Si_2$.

4. CONCLUSION

We have performed a comparative study of thermodynamic, magnetic and transport measurements on the two clean, stoichiometric and isostructural HF compounds $CeNi_2Ge_2$ and $YbRh_2Si_2$ which have been tuned into

quantum criticality by magnetic fields. Whereas $YbRh_2Si_2$ shows very weak AF order at $T_N = 70$ mK, suppressed by a tiny critical field $B_c = 0.06$ T, $CeNi_2Ge_2$ is located almost directly at the QCP ($B_c \approx 0$). We have used magnetic fields $b > 0$ ($b = B - B_c$) to induce a FL state in both materials and followed the field dependence of the QP mass being proportional to $\gamma_0(b)$ and QP-QP scattering cross section (proportional to $A(b)$) upon approaching the QCP by reducing $b \to 0$. For $CeNi_2Ge_2$ the evolution of both properties is in perfect agreement with the predictions of the 3D-SDW scenario, whereas for $YbRh_2Si_2$ the observed linear T-dependence of the electrical resistivity at $b = 0$ as well as the $1/b$ divergence of $A(b)$ would fit the SDW prediction only by assuming truly 2D critical spinfluctuations that render the entire Fermi surface "hot." The same scenario, however, predicts a logarithmic divergence of the QP mass at the QCP,[33] i.e., $C(T)/T \propto (-\ln T)$ at $b = 0$ and $\gamma_0(b) \propto (-\ln b)$ in the field-induced FL state. Very recently, careful specific heat experiments on $YbRh_2(Si_{1-x}Ge_x)_2$ with a (nominal) Ge-concentration of $x = 0.05$ (Ref. 34) for which T_N and B_c ($\perp c$) are reduced by a slight volume expansion to 20 mK and 0.027 T, respectively, have been performed.[35] At $b = 0$ a power-law divergence $C(T)/T \propto T^{-1/3}$ is observed below about 0.5 K. Additionally, $\gamma_0(b)$ in the field-induced LFL state for $b > 0$ diverges as $b^{-1/3}$ for fields lower than 0.5 T. The stronger than logarithmic mass divergence is incompatible with the SDW scenario. The latter predicts the "Kadowaki–Woods" ratio, K, to divergence as $K_{SDW} \propto (b \ln^2(b))^{-1}$. A truly constant K as found above $B = 0.5$ T in $YbRh_2Si_2$ (see inset Fig. 8) would indicate that the scattering amplitude remains local in the approach to the QCP. The weak field dependence $K \propto b^{-1/3}$ observed for $YbRh_2(Si_{0.95}Ge_{0.05})_2$ for $b \to 0$ implies that the characteristic length scale of the scattering amplitude renormalizes more slowly than expected by the SDW scenario and thus favors a locally-critical scenario for $YbRh_2Si_2$ (Ref. 35). According to the model by Si *et al.* (Ref. 6), the local QCP occurs for systems with strongly anisotropic, i.e., quasi-2D critical spinfluctuations and results in the emergence of spatially local critical excitations that co-exist with the spatially extended critical spin fluctuations. Thus, to understand the different behaviors observed for $CeNi_2Ge_2$ and $YbRh_2Si_2$ one would assume the magnetic fluctuations in the relevant energy range to be 3D for the former and 2D for the latter system. For $CeNi_2Ge_2$ recent inelastic neutron scattering experiments determined the critical fluctuations and found them to behave 3D, with no indications for a 2D-like anisotropy.[36] Similar experiments on $YbRh_2Si_2$ have not been performed yet.

To conclude, tuning the quantum critical points in $CeNi_2Ge_2$ and $YbRh_2Si_2$ by magnetic fields revealed that for the former system can be well described within the itinerant 3D-SDW model, whereas a locally

critical model seems to be appropriate for the latter system. For both systems, the quantum-critical behavior observed at low magnetic fields is well separated from a high-field scale at which the HF state is suppressed by a full polarization of the magnetic moments.

ACKNOWLEDGMENTS

We are grateful to P. Coleman, C. Pépin, and Q. Si for stimulating discussions. Work in Dresden has been supported in part by the Fonds der Chemischen Industrie.

REFERENCES

1. G. R. Stewart, *Rev. Mod. Phys.* **73**, 797 (2001).
2. P. Coleman, C. Pépin, Q. Si, and R. Ramazashvili, *J. Phys. Cond. Mat.* **13**, R723 (2001).
3. J. A. Hertz, *Phys. Rev. B* **14**, 1165 (1976).
4. A. J. Millis, *Phys. Rev. B* **48**, 7183 (1993).
5. T. Moriya and T. Takimoto, *J. Phys. Soc. Jpn.* **64**, 960 (1995).
6. Q. Si, S. Rabello, K. Ingersent, and J. L. Smith, *Nature* **413**, 804 (2001).
7. H. v. Löhneysen, *J. Phys. Cond. Mat.* **8**, 9689 (1996).
8. A. Rosch, A. Schröder, O. Stockert, and H. v. Löhneysen, *Phys. Rev. Lett.* **79**, 159 (1997).
9. A. Schröder, G. Aeppli, R. Coldea, M. Adams, O. Stockert, H. v. Löhneysen, E. Bucher, R. Ramazashvili, and P. Coleman, *Nature* **407**, 351 (2000).
10. P. Gegenwart, F. Kromer, M. Lang, G. Sparn, C. Geibel, and F. Steglich, *Phys. Rev. Lett.* **82**, 1293 (1999).
11. O. Trovarelli, C. Geibel, S. Mederle, C. Langhammer, F. M. Grosche, P. Gegenwart, M. Lang, G. Sparn, and F. Steglich, *Phys. Rev. Lett.* **85**, 626 (2000).
12. G. Knopp, A. Loidl, R. Caspary, U. Gottwick, C. D. Bredl, H. Spille, F. Steglich, and A. P. Murani, *J. Magn. Magn. Matter.* **74**, 341 (1988).
13. G. Knebel, M. Brando, J. Hemberger, M. Nicklas, W. Trinkl, and A. Loidl, *Phys. Rev. B* **59**, 12390 (1999).
14. P. Haen, J. Flouquet, F. Lapierre, P. Lejay, and G. Remenyi, *J. Low. Temp. Phys.* **67**, 391 (1987).
15. Y. Aoki, J. Urakawa, H. Sugawara, H. Sato, T. Fukuhara, and K. Maezawa, *J. Phys. Soc. Jpn.* **66**, 2993 (1997).
16. S. Koerner, E.-W. Scheidt, T. Schreiner, K. Heuser, and G. R. Stewart, *J. Low Temp. Phys.* **121**, 105 (2001).
17. F. Steglich, N. Sato, T. Tayama, T. Lühmann, C. Langhammer, P. Gegenwart, P. Hinze, C. Geibel, M. Lang, G. Sparn, and W. Assmus, *Physica C* **341–348**, 691 (2000).
18. T. Cichorek, C. Geibel, N. Carocca-Canales, T. Lühmann, P. Gegenwart, and F. Steglich, *Acta Phys. Pol. B* **34**, 371 (2003).
19. P. Gegenwart, P. Hinze, C. Geibel, M. Lang, and F. Steglich, *Physica B* **281–282**, 5 (2000).
20. F. M. Grosche, P. Agerwal, S. R. Julian, N. J. Wilson, R. K. W. Haselwimmer, S. J. S. Lister, N. D. Mathur, F. V. Carter, S. S. Saxena, and G. G. Lonzarich, *J. Phys. Cond. Mat.* **12** L533 (2000).
21. D. Braithwaite, T. Fukuhara, A. Demuer, I. Sheikin, S. Kambe, J.-P. Brison, K. Maezawa, T. Naka, and J. Flouquet, *J. Phys. Cond. Mat.* **12**, 1339 (2000).
22. T. Fukuhara, K. Maezawa, H. Ohkuni, J. Sakurai, H. Sato, H. Azuma, K. Sugiyama, Y. Ônuki, and K. Kindo, *J. Phys. Soc. Jpn.* **65**, 1559 (1996).

23. K. Heuser, E.-W. Scheidt, T. Schreiner, and G. R. Stewart, *Phys. Rev. B* **57**, R4198 (1998).
24. K. Heuser, E.-W. Scheidt, T. Schreiner, and G. R. Stewart, *Phys. Rev. B* **58**, R15959 (1998).
25. S. Seuring, K. Heuser, E.-W. Scheidt, T. Schreiner, E. Bauer, and G. R. Stewart, *Physica B* **281–282**, 374 (2000).
26. O. Trovarelli, C. Geibel, C. Langhammer, S. Mederle, P. Gegenwart, F. M. Grosche, M. Lang, G. Sparn, and F. Steglich, *Physica B* **281–282**, 372 (2000).
27. J. Custers, P. Gegenwart, C. Geibel, F. Steglich, T. Tayama, O. Trovarelli, and N. Harrison, *Act. Phys. Pol. B* **32**, 3221 (2001).
28. Y. Tokiwa, P. Gegenwart, F. Weickert, J. Custers, J. Ferstl, C. Geibel, and F. Steglich, *Proc. ICM Roma 2003,* to be published.
29. P. Gegenwart, J. Custers, C. Geibel, K. Neumaier, T. Tayama, K. Tenya, O. Trovarelli, and F. Steglich, *Phys. Rev. Lett.* **89**, 056402 (2002).
30. K. Ishida, D. E. MacLaughlin, O. O. Bernal, R. H. Heffner, G. J. Nieuwenhuys, O. Trovarelli, C. Geibel, and F. Steglich, *Physica B* **326**, 403 (2003).
31. K. Ishida, K. Okamoto, Y. Kawasaki, Y. Kitaoka, O. Trovarelli, C. Geibel, and F. Steglich, *Phys. Rev. Lett.* **89**, 107202 (2002).
32. K. Kadowaki and S. B. Woods, *Sol. St. Com.* **58**, 507 (1986).
33. I. Paul and G. Kotliar, *Phys. Rev. B* **64**, 184414 (2001).
34. O. Trovarelli, J. Custers, P. Gegenwart, C. Geibel, P. Hinze, S. Mederle, G. Sparn, and F. Steglich, *Physica B* **312–313**, 401 (2002).
35. J. Custers, P. Gegenwart, H. Wilhelm, K. Neumaier, Y. Tokiwa, O. Trovarelli, C. Geibel, C. Pépin, and P. Coleman, *Nature* **424**, 524 (2003).
36. H. Kadowaki, T. Fukuhara, and K. Maezawa, *Act. Phys. Pol. B* **34**, 375 (2003).